Multiscale materials science - a mathematical approach to the role of defects and uncertainty

Claude Le Bris
ECOLE NATIONALE DES PONTS ET CHAUSSEES

08/17/2016
Final Report

REPORT DOCUMENTATION PAGE

Form Approved
OMB No. 0704-0188

The public reporting burden for this collection of information is estimated to average 1 hour per response, including the time for reviewing instructions, searching existing data sources, gathering and maintaining the data needed, and completing and reviewing the collection of information. Send comments regarding this burden estimate or any other aspect of this collection of information, including suggestions for reducing the burden, to Department of Defense, Executive Services, Directorate (0704-0188).   Respondents should be aware that notwithstanding any other provision of law, no person shall be subject to any penalty for failing to comply with a collection of information if it does not display a currently valid OMB control number.
PLEASE DO NOT RETURN YOUR FORM TO THE ABOVE ORGANIZATION.

1. REPORT DATE *(DD-MM-YYYY)* 28-10-2016	2. REPORT TYPE Final	3. DATES COVERED *(From - To)* 01 Apr 2013 to 31 Mar 2016

4. TITLE AND SUBTITLE Multiscale materials science - a mathematical approach to the role of defects and uncertainty	5a. CONTRACT NUMBER
	5b. GRANT NUMBER FA8655-13-1-3061
	5c. PROGRAM ELEMENT NUMBER 61102F
6. AUTHOR(S) Claude Le Bris, Frederic Legoll	5d. PROJECT NUMBER
	5e. TASK NUMBER
	5f. WORK UNIT NUMBER

7. PERFORMING ORGANIZATION NAME(S) AND ADDRESS(ES) ECOLE NATIONALE DES PONTS ET CHAUSSEES 6, AVENUE BLAISE PASCAL 6 ET 8 CITE DESCARTES CHAMPS SUR MARNE, 77420 FR	8. PERFORMING ORGANIZATION REPORT NUMBER

9. SPONSORING/MONITORING AGENCY NAME(S) AND ADDRESS(ES) EOARD Unit 4515 APO AE 09421-4515	10. SPONSOR/MONITOR'S ACRONYM(S) AFRL/AFOSR IOE
	11. SPONSOR/MONITOR'S REPORT NUMBER(S) AFRL-AFOSR-UK-TR-2016-0034

12. DISTRIBUTION/AVAILABILITY STATEMENT
A DISTRIBUTION UNLIMITED: PB Public Release

13. SUPPLEMENTARY NOTES

14. ABSTRACT
The bottom line of our work is to develop affordable numerical methods in the context of heterogeneous,possibly random, materials. In this report, we first consider a multiscale advection-diffusion problem on a perforated domain, in the convection-dominated regime. We show how to adapt two classical methods, MsFEM type approaches and stabilized type techniques (e.g. the Streamline Upwind Petrov-Galerkin [SUPG] method), in a unified single approach to efficiently solve these multiscale advection-diffusion problems. Numerical results are shown, and a comparison amongst the MsFEM approaches is given.

15. SUBJECT TERMS
multiscale modeling, uncertainty quantification, prognosis, numerical simulation, damage modeling, EOARD

16. SECURITY CLASSIFICATION OF:			17. LIMITATION OF ABSTRACT	18. NUMBER OF PAGES	19a. NAME OF RESPONSIBLE PERSON FOLEY, JASON
a. REPORT Unclassified	b. ABSTRACT Unclassified	c. THIS PAGE Unclassified	SAR	36	19b. TELEPHONE NUMBER *(Include area code)* 011-44-1895-616036

Standard Form 298 (Rev. 8/98)
Prescribed by ANSI Std. Z39.18

Contract FA 8655-13-1-3061

Multiscale materials science: a mathematical approach
to the role of defects and uncertainty

Report 2016 to the European Office of
Aerospace Research and Development (EOARD)

C. Le Bris, F. Legoll, S. Lemaire and F. Madiot

June 2016

Contents

Executive Summary

We report here on the work performed during the third year (April 2015 - March 2016) of the contract FA 8655-13-1-3061 on *Multiscale materials science: a mathematical approach to the role of defects and uncertainty.*

The bottom line of our work is to develop *affordable numerical methods* in the context of *heterogeneous*, possibly *random*, materials.

Many partial differential equations of materials science indeed involve highly oscillatory coefficients and thus small length-scales. When the microstructure of the materials is periodic, or random and statistically homogeneous, homogenization theory can be used, and allows to appropriately define averaged equations from the original oscillatory equations. When no such structural assumption (e.g. periodicity) on the materials microstructure can be made, homogenization theory still holds, but does not provide any explicit formulae amenable (even possibly after some approximation) to numerical computation. One possibility is then to directly address the original problem (rather than passing to the limit of infinite scale separation), and to use dedicated numerical approaches for such multiscale problems, such as the Multiscale Finite Element Method (MsFEM).

In this report, we first consider a multiscale advection-diffusion problem on a perforated domain, in the convection-dominated regime (see Section 1). There are two small scales in the problem. The first small scale is the size of the perforations, which is of the same order of magnitude as the distance between two neighboring perforations. The second small scale is related to the ratio between the diffusion and the convection coefficients. In addition to the difficulty owing to the presence of different scales, the strong convection is also a source of potential instabilities. Taken *separately*, each phenomenon can be addressed by classical approaches: MsFEM type approaches and stabilized type techniques (e.g. the Streamline Upwind Petrov-Galerkin (SUPG) method), respectively. We show here how to adapt these two methods in a unified single approach to efficiently solve multiscale advection-diffusion problems set on perforated domains, in the convection-dominated regime.

The problem we consider here is similar in spirit to the multiscale advection-diffusion problem considered in [EOARD3, EOARD6], except that there, the multiscale nature of the problem was stemming from the fact that the diffusion coefficient in the problem was highly oscillatory. Here, the multiscale nature of the problem originates from the geometry of the domain on which the problem is posed.

Recall that the MsFEM method consists of:

- an "offline" stage, where highly oscillatory basis functions are numerically computed as solutions of local problems (that mimick in a suitable way the reference problem on a subdomain). These basis functions are thus expected to be well-adapted to the problem at hand.

- an "online" stage, where a Galerkin approximation of the reference problem is solved. The approximation is performed in the finite dimensional space spanned by the basis functions computed in the prior offline stage.

In this work, we compare different numerical approaches:

- A first approach (denoted Adv-MsFEM below) is to take into account *both* the diffusion term and the convection term in the definition of the basis functions (see (7)–(8) below).

- A second approach (denoted MsFEM below) is to *only* take into account the diffusion term in the definition of the basis functions (see (10)–(11) below).

In the online stage, both approaches may be stabilized, or not, using e.g. the SUPG technique (see (13) and (19) below).

Preliminary results have been obtained. Our partial conclusions are as follows. For identical discretization parameters, the Adv-MsFEM and its stabilized variant (the Stab-Adv-MsFEM approach) provide results with similar accuracy, which are better than those obtained using the MsFEM or the Stab-MsFEM approaches. The costs of the non-stabilized variants are similar, and smaller than the costs of the stabilized variants, due to the need for the latter to assemble the stabilization terms. For the problem of interest here, the method of choice seems to be the Adv-MsFEM approach, although more comprehensive numerical tests are needed to confirm this.

This ongoing work is being reported on in [EOARD4]. It is performed by Claude Le Bris (PI), Frédéric Legoll (Co-PI) and François Madiot (third year PhD student, see [EOARD7]), thanks to the specific support of EOARD to the research activity of our group. It is a follow-up of the work [EOARD3], described in [EOARD6], and of the work [EOARD2], described in [EOARD5].

We next describe in Section 2 some works related to the construction of coarse approximations for problems with highly oscillatory coefficients. Our aim

is to define and construct the best non-oscillating coefficient $\overline{A}$ (think e.g. of a constant coefficient) that is consistent, in a sense to be made precise, with the behavior of a heterogeneous material modelled by a highly oscillatory coefficient $A^\varepsilon(x)$. Such an approach can be considered as an alternative pathway to standard homogenization techniques when these latter are difficult to use in practice, in particular when information is missing on the coefficient $A^\varepsilon(x)$. Of course, modelling the material with $\overline{A}$ (rather than $A^\varepsilon(x)$) yields much more affordable approaches, since there is no fast frequency in that coefficient. A central question, of course intimately related to homogenization theory, is to construct in an efficient manner this best constant coefficient.

We focus here on the case when $A^\varepsilon(x)$ is random, which is a discriminating case where the standard homogenization approach is very expensive. We show below that, for an essentially identical computational cost compared to the standard homogenization approach, our approach allows us to compute a more accurate approximation of the solution u^ε to the highly oscillatory equation (both in L^2 and in H^1 norms). In contrast, it is less efficient for the approximation of the homogenized matrix $A_\star$.

This work has been expanded in [EOARD1] (it is also briefly described in [EOARD6]). It has been performed by Claude Le Bris (PI), Frédéric Legoll (Co-PI) and Simon Lemaire, a postdoc student fully funded by this contract and who joined our group from June 2014 to September 2015.

References authored by the investigators in the context of the contract

[EOARD1] C. Le Bris, F. Legoll and S. Lemaire, *On the best constant matrix approximating an oscillatory matrix-valued coefficient in divergence-form operators*, in preparation.

[EOARD2] C. Le Bris, F. Legoll and A. Lozinski, *An MsFEM type approach for perforated domains*, SIAM Multiscale Modeling and Simulation, vol. 12 (3), 1046-1077 (2014).

[EOARD3] C. Le Bris, F. Legoll and F. Madiot, *A numerical comparison of some Multiscale Finite Element approaches for convection-dominated problems in heterogeneous media*, arXiv preprint 1511.08453, submitted.

[EOARD4] C. Le Bris, F. Legoll and F. Madiot, *Multiscale Finite Element approaches for convection-dominated problems in perforated domains*, in preparation.

[EOARD5] C. Le Bris and F. Legoll, *Multiscale materials science: a mathematical approach to the role of defects and uncertainty*, EOARD Report 2014.

[EOARD6] C. Le Bris, F. Legoll, S. Lemaire and F. Madiot, *Multiscale materials science: a mathematical approach to the role of defects and uncertainty*, EOARD Report 2015.

[EOARD7] F. Madiot, *MsFEM-type approaches for advection-diffusion problems*, PhD Thesis, in preparation (defense expected Fall 2016).

Topics not reported on here but where the support of this EOARD grant has been acknowledged

[1] X. Blanc, C. Le Bris and F. Legoll, *Some variance reduction methods for numerical stochastic homogenization*, Philosophical Transactions of the Royal Society A, vol. 374 (2066), 20150168 (2016).

[2] E. Cancès, V. Ehrlacher, F. Legoll and B. Stamm, *An embedded corrector problem to approximate the homogenized coefficients of an elliptic equation*, C. R. Acad. Sci. Paris, Série I, vol. 353 (9), 801-806 (2015).

[3] Y. Efendiev, C. Kronsbein and F. Legoll, *Multi-Level Monte Carlo approaches for numerical homogenization*, SIAM Multiscale Modeling and Simulation, vol. 13 (4), 1107-1135 (2015).

[4] C. Le Bris and F. Legoll, *Examples of computational approaches to accommodate randomness in elliptic PDEs*, arXiv preprint 1604.05061, submitted.

[5] C. Le Bris, F. Legoll and F. Madiot, *Stabilisation de problèmes non coercifs via une méthode numérique utilisant la mesure invariante (Stabilization of non-coercive problems using the invariant measure)*, C. R. Acad. Sci. Paris, Série I, accepted for publication, available at

http://www.sciencedirect.com/science/article/pii/S1631073X16300814.

[6] C. Le Bris, F. Legoll and W. Minvielle, *Special Quasirandom Structures: a selection approach for stochastic homogenization*, Monte Carlo Methods and Applications, vol. 22 (1), 25-54 (2016).

[7] C. Le Bris, F. Legoll and F. Thomines, *Multiscale Finite Element approach for "weakly" random problems and related issues*, Mathematical Modelling and Numerical Analysis, vol. 48 (3), 815-858 (2014).

[8] F. Legoll and W. Minvielle, *A control variate approach based on a defect-type theory for variance reduction in stochastic homogenization*, SIAM Multiscale Modeling and Simulation, vol. 13 (2), 519-550 (2015).

[9] F. Legoll and F. Thomines, *On a variant of random homogenization theory: convergence of the residual process and approximation of the homogenized coefficients*, Mathematical Modelling and Numerical Analysis, vol. 48 (2), 347-386 (2014).

1 Multiscale advection-diffusion problems posed on perforated domains

As announced in the previous EOARD report [EOARD6], we describe here ongoing works concerned with multiscale advection-diffusion problems posed on perforated domains, in the convection-dominated regime. This problems brings together two difficulties we have already worked on:

- problems set on perforated domains, which we addressed (in a purely diffusive context) in [EOARD2].

- advection-diffusion problems posed on standard (i.e. non-perforated) domains, which we addressed during the PhD thesis [EOARD7] of François Madiot, whose research activity is partly funded by this Grant.

The work we describe here is a follow-up of these two works, with a strong practical motivation.

1.1 Introduction

We consider a bounded domain $\Omega \subset \mathbb{R}^d$ and a set B_ε of perforations within this domain. The perforations are supposedly small and in extremely large a number (so that they are close to each other). The parameter ε encodes the typically small distance between the perforations. We denote by $\Omega_\varepsilon = \Omega \setminus \overline{B_\varepsilon}$ the perforated domain (see Figure 1).
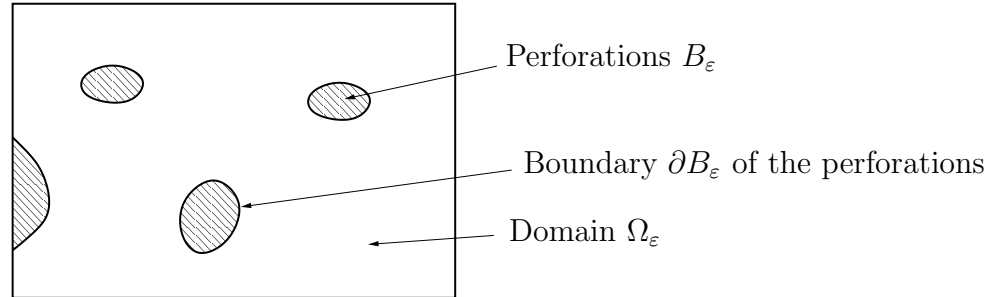
Figure 1: The domain Ω contains (possibly random) perforations B_ε. The perforated domain is $\Omega_\varepsilon = \Omega \setminus \overline{B_\varepsilon}$. The boundary of Ω_ε is the union of $\partial B_\varepsilon \cap \overline{\Omega_\varepsilon}$ (the part of the boundary of the perforations that is included in $\overline{\Omega_\varepsilon}$) and of $\partial\Omega \cap \overline{\Omega_\varepsilon}$.

7

The problem we consider reads

$$-\alpha\Delta u^\varepsilon + \frac{b(x/\varepsilon)}{\varepsilon} \cdot \nabla u^\varepsilon = f \ \text{ in } \Omega_\varepsilon, \qquad u^\varepsilon = 0 \ \text{ on } \partial\Omega_\varepsilon. \tag{1}$$

The homogeneous Dirichlet boundary condition (i.e. $u^\varepsilon = 0$) on the boundary of the perforations is an important feature of (1). It is motivated by the fact that (1) can be seen as a step toward the resolution of the Stokes problem on perforated domains. In that case, homogeneous Dirichlet boundary conditions on the perforations are typical for many applicative contexts.

The parameter α in (1) is a positive constant. The convection field b is assumed to be divergence-free. In the sequel, we assume that the ambient dimension is $d = 2$ and that $\Omega = (0,1)^2$.

Two comments are in order regarding the definition of problem (1).

First, note that we have scaled the convection term by a factor $1/\varepsilon$ in (1). In that regime, and assuming that the perforations are periodically located and that b is periodic, it can be shown that

$$\lim_{\varepsilon\to 0} \left\| u^\varepsilon - \varepsilon^2 \, w\left(\frac{\cdot}{\varepsilon}\right) f \right\|_{H^1(\Omega_\varepsilon)} = 0, \tag{2}$$

where the function w solves the so-called corrector problem

$$\begin{cases} -\alpha\Delta w + b \cdot \nabla w = 1 \ \text{ in } Y \setminus \overline{B}, \qquad w = 0 \quad \text{in } B, \\ y \mapsto w(y) \quad \text{is } Y\text{-periodic}, \end{cases}$$

where Y is the unit cell and B is the perforation of that unit cell. Through w, the asymptotic behavior of u^ε hence depends on the convection field b. In contrast, if we consider the problem

$$-\alpha\Delta v^\varepsilon + b(x/\varepsilon) \cdot \nabla v^\varepsilon = f \ \text{ in } \Omega_\varepsilon, \qquad v^\varepsilon = 0 \ \text{ on } \partial\Omega_\varepsilon, \tag{3}$$

where the convection term is *not* scaled by a factor $1/\varepsilon$, then (2) still holds but with w defined by

$$\begin{cases} -\alpha\Delta w = 1 \ \text{ in } Y \setminus \overline{B}, \qquad w = 0 \quad \text{in } B, \\ y \mapsto w(y) \quad \text{is } Y\text{-periodic}. \end{cases}$$

For asymptotically small ε, the solution v^ε to (3) can hence be well approximated by a quantity *independent* of the convection field. This suggests that, for ε small,

the effect of the convection is less critical (and thus less challenging to capture) than in the case of (1).

Second, we recall that, in [EOARD3] (see also [EOARD6]), we have considered the multiscale advection-diffusion problem

$$- \operatorname{div} \left[A^{\varepsilon}(x) \nabla u^{\varepsilon} \right] + b(x) \cdot \nabla u^{\varepsilon} = f \ \text{ in } \Omega, \qquad u^{\varepsilon} = 0 \ \text{ on } \partial \Omega, \qquad (4)$$

where the diffusion coefficient A^{ε} varies at the small scale ε, and where the convection vector field $b(x)$ is given and large. In some loose sense, the consideration of (4) is a preparatory step toward that of (1). For (4), boundary layers appear in localized subdomains of Ω. In contrast, for problem (1), boundary layers appear throughout the perforated domain Ω_{ε}. Again the effect of the convection is expected to be more critical.

Examples of applications of (1) include the (Navier-) Stokes equation in perforated media. The twofold difficulty of such problems lies in the presence of *two small scales* that we detail below. Efficient numerical approaches have been proposed to address either of the two difficulties, but not the two of them together:

(i) in the absence of convection (i.e. if $b = 0$ in (1)), the problem becomes a purely diffusive problem set on a multiscale perforated domain. This problem can be efficiently approximated by dedicated MsFEM approaches, such as the one we proposed in [EOARD2] (see also [EOARD5]), which is based on using Crouzeix-Raviart type basis functions. See Figure 2 for a representative example.

(ii) in the absence of perforations, the problem reads

$$-\alpha \Delta u + b(x) \cdot \nabla u = f \ \text{ in } \Omega, \qquad u = 0 \ \text{ on } \partial \Omega, \qquad (5)$$

and is again simple to treat using the now classical stabilization techniques for finite element methods (FEM). For example, the exact solution of (5), in the one-dimensional case, is shown on Figure 3 for b large. It is well-known that, unless the mesh size is smaller than the boundary layer width, classical P1 FEM perform poorly. The solution is not well approximated, not only within the boundary layer, but also away from it, because of numerical instabilities. Methods alternative to classical P1 FEM, known as stabilized approaches (e.g. the Streamline Upwind Petrov-Galerkin (SUPG) method), have been introduced long ago in the literature. They are very effective, as can be seen on Figure 3.
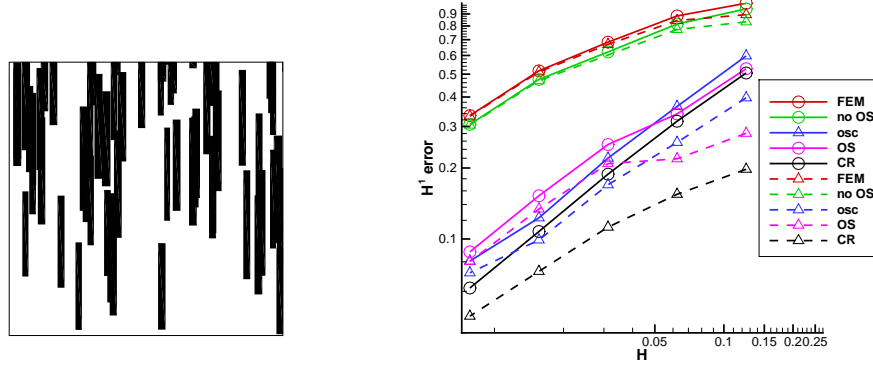
9

Figure 2: Left: an example of a domain with non-periodic perforations (represented in black). Right: relative errors with various approaches: FEM – the standard Q1 finite elements, no OS – MsFEM with linear boundary conditions, osc – MsFEM with oscillatory boundary conditions, OS – MsFEM with oversampling, CR – the Crouzeix-Raviart type MsFEM approach we propose. Results for all these methods are represented by solid lines. The dashed lines correspond to the variants of these methods where we enrich the finite element spaces using bubble functions. See [EOARD2] for details.
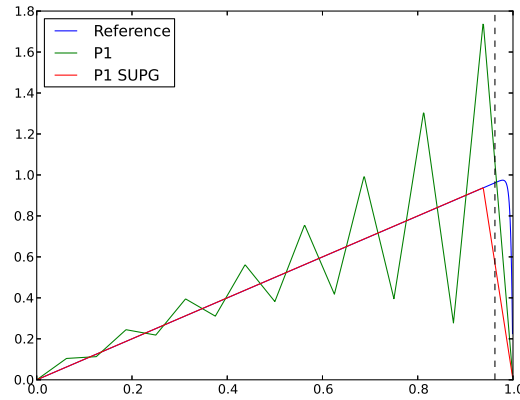

Figure 3: In blue, the exact solution to (5) for $\Omega = (0, 1)$ and $b = 200$. In green (resp. red), the numerical solution obtained by a P1 (resp. stabilized P1) approach with $H = 0.08$. The P1 solution shows spurious oscillations while the P1 SUPG solution is very accurate except in the boundary layer.

10

In the sequel, we focus on problem (1). The question is to design an efficient MsFEM approach for that problem. It is unclear whether it needs to be stabilized and how to achieve this in the most effective way. We report below on the preliminary results that we have obtained, and refer to [EOARD4, EOARD7] for comprehensive results.

1.2 Numerical approaches

We recall that the variational formulation associated to (1) consists in finding $u^\varepsilon \in H_0^1(\Omega_\varepsilon)$ such that

$$\forall v \in H_0^1(\Omega_\varepsilon), \quad \mathcal{A}_\varepsilon(u^\varepsilon, v) = F_\varepsilon(v), \tag{6}$$

where

$$\mathcal{A}_\varepsilon(u, v) = \alpha \int_{\Omega_\varepsilon} \nabla v \cdot \nabla u + \left(\frac{b(x/\varepsilon)}{\varepsilon} \cdot \nabla u \right) v \quad \text{and} \quad F_\varepsilon(v) = \int_{\Omega_\varepsilon} f \, v.$$

Following the spirit of the MsFEM approaches, our aim is to introduce, at the coarse scale, a finite-dimensional approximation space spanned by suitably chosen basis functions, and to consider the Galerkin approximation of (6) in that space. We describe here the different variants we have considered, before turning in Section 1.3 to the obtained numerical results.

We mesh Ω, and denote $\mathcal{T}_H$ the set of triangles $\mathbf{K} \subset \Omega$. We denote by $\mathcal{E}_H$ the set of all the internal edges of $\mathcal{T}_H$. Note that we mesh Ω and not the perforated domain Ω_ε. This allows us to use coarse elements (independently of the fine scale present in the geometry of Ω_ε), and leaves us with a lot of flexibility. The mesh does not have to be consistent with the perforations B_ε. Some nodes may lie in B_ε, and, likewise, some edges may intersect B_ε. We assume in the sequel that no element $\mathbf{K} \in \mathcal{T}_H$ and no internal edge $E \in \mathcal{E}_H$ is a subset of the perforations B_ε (recall that the mesh is coarse while the perforations are small, so this assumption is easily satisfied in practice).

In the vein of our earlier work [EOARD2] on MsFEM approaches for diffusive problems set on perforated domains, we consider MsFEM basis functions defined with Crouzeix-Raviart type boundary conditions. For purely diffusive problems, they have proved to be extremely flexible.

We now briefly present our four numerical approaches. For each of them, the basis set consists of two types of functions:

11

- a function $\Phi^{\varepsilon,E} \in \mathcal{E}_H$ associated to each edge E of the mesh, as is usual for Crouzeix-Raviart type approaches;

- a function $\Psi^{\varepsilon,\mathbf{K}}$ associated to each element $\mathbf{K} \in \mathcal{T}_H$ of the mesh, which vanishes (in a weak way) on the edges of that element. Such functions are called bubble functions in what follows. In the context of purely diffusive problems, the need to use such basis functions for problems posed on perforated domains has been detailed in our previous work [EOARD2], and can be observed on Figure 2. In the present context of convection-diffusion problems, we have also considered the variant where we do not include bubble functions in the basis sets. Results are shown on Figure 4 for the Adv-MsFEM variant described in Section 1.2.1 below (similar results have been obtained with the other MsFEM variants). As for our previous work [EOARD2], the interest of adding bubble functions to the basis set is evident.
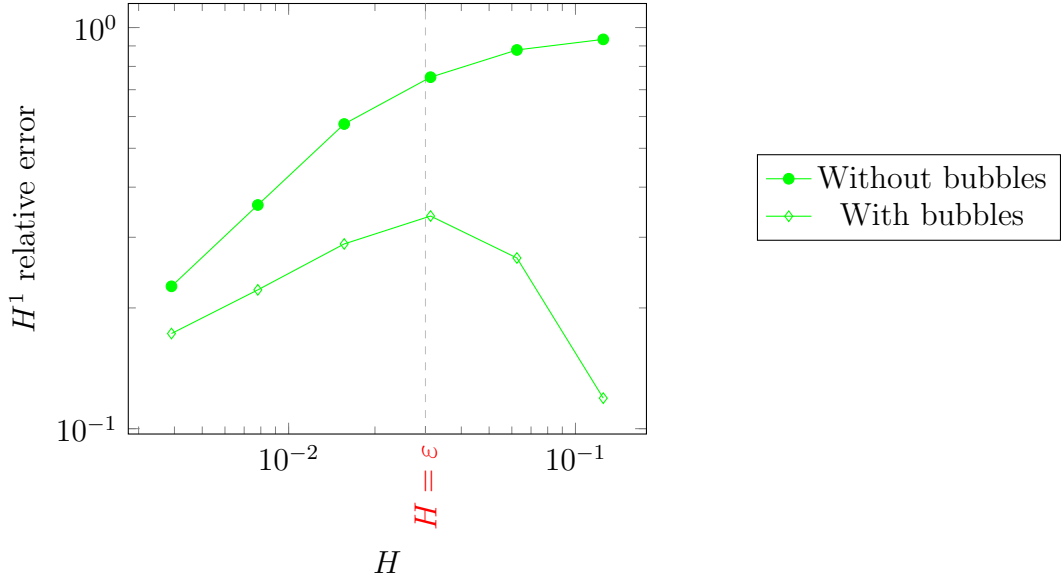

Figure 4: Relative H^1 error (as defined by (20) below) for the Adv-MsFEM variant ($\alpha = 1/4$, $\varepsilon = 0.03$; the vertical dashed line represents the region where $H = \varepsilon$), when including or not bubble functions in the basis set.

12

1.2.1 Adv-MsFEM variant

In that variant, for each $\mathbf{K} \in \mathcal{T}_H$, we solve the local problem

$$-\alpha \Delta \Psi^{\varepsilon,\mathbf{K}} + \frac{b(x/\varepsilon)}{\varepsilon} \cdot \nabla \Psi^{\varepsilon,\mathbf{K}} = 1 \ \text{ in } \mathbf{K} \setminus \overline{B_\varepsilon}, \qquad \Psi^{\varepsilon,\mathbf{K}} = 0 \ \text{ in } B_\varepsilon, \qquad (7)$$

with the so-called Crouzeix-Raviart boundary conditions: for each edge Γ_i of $\mathbf{K}$, we set $\displaystyle\int_{\Gamma_i} \Psi^{\varepsilon,\mathbf{K}} = 0$ and $n \cdot \nabla \Psi^{\varepsilon,\mathbf{K}} = \lambda_i$ on Γ_i for some constant λ_i. The basis functions $\Psi^{\varepsilon,\mathbf{K}}$ are called bubbles in what follows.

Second, for each internal edge $E \in \mathcal{E}_H$, we denote by $\mathbf{K}_E^1$ and $\mathbf{K}_E^2$ the two triangles sharing this edge, set $\mathbf{K}_E := \mathbf{K}_E^1 \cup \mathbf{K}_E^2$ (see Figure 5), and consider $\Phi^{\varepsilon,E}$ solution to

$$\begin{cases} -\alpha \Delta \Phi^{\varepsilon,E} + \dfrac{b(x/\varepsilon)}{\varepsilon} \cdot \nabla \Phi^{\varepsilon,E} = 0 \text{ in } \mathbf{K}_E^1 \setminus \overline{B_\varepsilon}, \\[2mm] -\alpha \Delta \Phi^{\varepsilon,E} + \dfrac{b(x/\varepsilon)}{\varepsilon} \cdot \nabla \Phi^{\varepsilon,E} = 0 \text{ in } \mathbf{K}_E^2 \setminus \overline{B_\varepsilon}, \\[2mm] \Phi^{\varepsilon,E} = 0 \text{ in } B_\varepsilon, \end{cases} \qquad (8)$$

with, for each edge $E' \subset \partial \mathbf{K}_E$, $\displaystyle\int_{E'} \Phi^{\varepsilon,E} = 0$ and $n \cdot \nabla \Phi^{\varepsilon,E} = \lambda_{E'}$ on E' for some constant $\lambda_{E'}$ and $\displaystyle\int_E \Phi^{\varepsilon,E} = 1$ and $n \cdot \nabla \Phi^{\varepsilon,E} = \lambda_E$ on E for some constant λ_E (with an a priori different constant on the two sides of E).
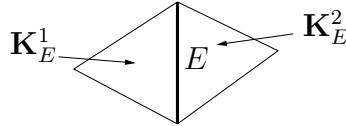
Figure 5: Construction of $\Phi^{\varepsilon,E}$ following (8).

The Adv-MsFEM approximation space is

$$V_H^{\varepsilon,Adv} = \text{Span} \left\{ \Phi^{\varepsilon,E}, \ \Psi^{\varepsilon,\mathbf{K}}, \quad E \in \mathcal{E}_H, \ \ \mathbf{K} \in \mathcal{T}_H \right\}. \qquad (9)$$

The Adv-MsFEM method is the standard Galerkin approximation of (6) on $V_H^{\varepsilon,Adv}$:

Find $u_H^\varepsilon \in V_H^{\varepsilon,Adv}$ such that, $\forall v_H^\varepsilon \in V_H^{\varepsilon,Adv}$, $\ \mathcal{A}_\varepsilon^H(u_H^\varepsilon, v_H^\varepsilon) = F_\varepsilon(v_H^\varepsilon)$,

13

where

$$\mathcal{A}_\varepsilon^H(u,v) = \alpha \sum_{\mathbf{K} \in \mathcal{T}_H} \int_{\mathbf{K} \cap \Omega_\varepsilon} \nabla v \cdot \nabla u + \sum_{\mathbf{K} \in \mathcal{T}_H} \int_{\mathbf{K} \cap \Omega_\varepsilon} \left(\frac{b(x/\varepsilon)}{\varepsilon} \cdot \nabla u \right) v.$$

1.2.2 Classical MsFEM variant

The basis functions of the Adv-MsFEM variant presented above depend on the convection field b. Thus, if b changes, the basis set has to be recomputed. This may be expensive. We explore here the possibility of a MsFEM variant in which the basis functions do *not* depend on b. This variant is henceforth called the MsFEM variant.

For each $\mathbf{K} \in \mathcal{T}_H$, we solve the local problem

$$-\alpha \Delta \Psi_0^{\varepsilon,\mathbf{K}} = 1 \ \ \text{in } \mathbf{K} \setminus \overline{B_\varepsilon}, \qquad \Psi_0^{\varepsilon,\mathbf{K}} = 0 \ \ \text{in } B_\varepsilon, \tag{10}$$

with the same boundary conditions as for (7). In addition, for each internal edge E, we consider $\Phi_0^{\varepsilon,E}$ solution to (see Figure 5 for notations)

$$\begin{cases} -\alpha \Delta \Phi_0^{\varepsilon,E} = 0 \text{ in } \mathbf{K}_E^1 \setminus \overline{B_\varepsilon}, \\ -\alpha \Delta \Phi_0^{\varepsilon,E} = 0 \text{ in } \mathbf{K}_E^2 \setminus \overline{B_\varepsilon}, \\ \Phi_0^{\varepsilon,E} = 0 \text{ in } B_\varepsilon, \end{cases} \tag{11}$$

with the same boundary conditions as for (8).

The MsFEM approximation space is

$$V_H^\varepsilon = \text{Span} \left\{ \Phi_0^{\varepsilon,E}, \ \Psi_0^{\varepsilon,\mathbf{K}}, \quad E \in \mathcal{E}_H, \ \ \mathbf{K} \in \mathcal{T}_H \right\}. \tag{12}$$

The MsFEM method is the standard Galerkin approximation of (6) on V_H^ε:

Find $u_H^\varepsilon \in V_H^\varepsilon$ such that, $\forall v_H^\varepsilon \in V_H^\varepsilon, \ \ \mathcal{A}_\varepsilon^H(u_H^\varepsilon, v_H^\varepsilon) = F_\varepsilon(v_H^\varepsilon).$

In the numerical results described below (see Section 1.3), we will observe that this approach performs poorly when α decreases, that is when convection increasingly dominates. There is thus a need for stabilization.

14

1.2.3 Stab-MsFEM variant

We use the same approximation space V_H^ε as in the classical MsFEM variant of Section 1.2.2, but we modify the bilinear form by adding stabilization terms. The problem consists in finding $u_H^\varepsilon \in V_H^\varepsilon$ such that

$$\forall v_H^\varepsilon \in V_H^\varepsilon, \quad \mathcal{A}_\varepsilon^H(u_H^\varepsilon, v_H^\varepsilon) + \mathcal{A}_{\text{stab}}(u_H^\varepsilon, v_H^\varepsilon) = F_\varepsilon(v_H^\varepsilon) + F_{\text{stab}}(v_H^\varepsilon), \quad (13)$$

where

$$\mathcal{A}_{\text{stab}}(u_H^\varepsilon, v_H^\varepsilon) = \sum_{\mathbf{K} \in \mathcal{T}_H} \int_{\mathbf{K} \cap \Omega_\varepsilon} \tau_{\mathbf{K}}(x) \left[\mathcal{L} u_H^\varepsilon \right] \left[\frac{b(x/\varepsilon)}{\varepsilon} \cdot \nabla v_H^\varepsilon \right] \quad (14)$$

$$F_{\text{stab}}(v_H^\varepsilon) = \sum_{\mathbf{K} \in \mathcal{T}_H} \int_{\mathbf{K} \cap \Omega_\varepsilon} \tau_{\mathbf{K}}(x) \, f \, \frac{b(x/\varepsilon)}{\varepsilon} \cdot \nabla v_H^\varepsilon. \quad (15)$$

In the definition of $\mathcal{A}_{\text{stab}}$ and F_{stab}, $\tau_{\mathbf{K}}$ is a stabilization parameter, the value of which is here chosen to be

$$\tau_{\mathbf{K}}(x) = \frac{H}{2|b(x/\varepsilon)/\varepsilon|} \left(\coth(\text{Pe}(x)\, H) - \frac{1}{\text{Pe}(x)\, H} \right), \quad \text{Pe}(x) = \frac{|b(x/\varepsilon)|}{2\varepsilon\alpha},$$

and

$$\mathcal{L} u = -\alpha \Delta u + \frac{b(x/\varepsilon)}{\varepsilon} \cdot \nabla u$$

is the operator corresponding to the problem at hand.

The method is, as is well known, strongly consistent. In view of the definition (10)–(11)–(12) of V_H^ε, any $u_H^\varepsilon \in V_H^\varepsilon$ can be written as

$$u_H^\varepsilon(x) = \sum_{E \in \mathcal{E}_H} U_E \, \Phi_0^{\varepsilon, E}(x) + \sum_{\mathbf{K} \in \mathcal{T}_H} U_{\mathbf{K}} \, \Psi_0^{\varepsilon, \mathbf{K}}(x),$$

and thus, for any u_H^ε and v_H^ε in V_H^ε, we have that

$$\mathcal{A}_{\text{stab}}(u_H^\varepsilon, v_H^\varepsilon) = \mathcal{A}_{\text{upw}}(u_H^\varepsilon, v_H^\varepsilon) \quad (16)$$

where

$$\mathcal{A}_{\text{upw}}(u_H^\varepsilon, v_H^\varepsilon) = \sum_{\mathbf{K} \in \mathcal{T}_H} \int_{\mathbf{K} \cap \Omega_\varepsilon} \tau_{\mathbf{K}}(x) \left(\frac{b(x/\varepsilon)}{\varepsilon} \cdot \nabla u_H^\varepsilon \right) \left(\frac{b(x/\varepsilon)}{\varepsilon} \cdot \nabla v_H^\varepsilon \right)$$

$$+ \sum_{\mathbf{K} \in \mathcal{T}_H} U_{\mathbf{K}} \int_{\mathbf{K} \cap \Omega_\varepsilon} \tau_{\mathbf{K}}(x) \left(\frac{b(x/\varepsilon)}{\varepsilon} \cdot \nabla v_H^\varepsilon \right). \quad (17)$$

15

In practice however, we only know discrete approximations $\Psi_{0,h}^{\varepsilon,\mathbf{K}}$ and $\Phi_{0,h}^{\varepsilon,E}$, on a fine mesh $\mathbf{K}_h$, of the solutions $\Psi_0^{\varepsilon,\mathbf{K}}$ and $\Phi_0^{\varepsilon,E}$ to (10) and (11), respectively. Put differently, we manipulate

$$V_{H,h}^{\varepsilon} = \mathrm{Span}\left\{\Phi_{0,h}^{\varepsilon,E},\ \Psi_{0,h}^{\varepsilon,\mathbf{K}},\quad E \in \mathcal{E}_H,\quad \mathbf{K} \in \mathcal{T}_H\right\}$$

instead of V_H^{ε}. It follows that, when we use a $\mathbb{P}^1$ approximation on a fine mesh $\mathbf{K}_h$ for the local problems (10) and (11), $\nabla u_{H,h}^{\varepsilon}$ may be discontinuous at the edges of the mesh $\mathbf{K}_h$, thus $-\Delta u_{H,h}^{\varepsilon} \notin L_{\mathrm{loc}}^1(\mathbf{K})$ and eventually $\mathcal{A}_{\mathrm{stab}}(u_{H,h}^{\varepsilon}, v_{H,h}^{\varepsilon})$ is ill-defined.

We may consider at least two ways to circumvent that difficulty. First, we may define the stabilization term as

$$\widetilde{\mathcal{A}}_{\mathrm{stab}}(u_{H,h}^{\varepsilon}, v_{H,h}^{\varepsilon}) = \sum_{\mathbf{K}\in\mathcal{T}_H}\sum_{\kappa\subset\mathbf{K}_h}\int_{\kappa\cap\Omega_\varepsilon}\tau_{\mathbf{K}}(x)\left[\mathcal{L}u_{H,h}^{\varepsilon}\right]\ \left[\frac{b(x/\varepsilon)}{\varepsilon}\cdot\nabla v_{H,h}^{\varepsilon}\right].$$

We then obtain a strongly consistent stabilized method. We will however not proceed in this direction and favor an alternate approach, to which we now turn.

Based upon the observation (16) for the "ideal" space V_H^{ε}, we may use the stabilization term (17) rather than (14). In contrast to (14), the quantity (17) is also well defined on $V_{H,h}^{\varepsilon}$. The Stab-MsFEM variant we employ is hence defined by the following variational formulation: find $u_{H,h}^{\varepsilon} \in V_{H,h}^{\varepsilon}$ such that

$$\forall v_{H,h}^{\varepsilon} \in V_{H,h}^{\varepsilon},\quad \mathcal{A}_{\varepsilon}^{H}(u_{H,h}^{\varepsilon}, v_{H,h}^{\varepsilon}) + \mathcal{A}_{\mathrm{upw}}(u_{H,h}^{\varepsilon}, v_{H,h}^{\varepsilon}) = F_{\varepsilon}(v_{H,h}^{\varepsilon}) + F_{\mathrm{stab}}(v_{H,h}^{\varepsilon}).\quad (18)$$

We emphasize that employing that stabilization comes at a price: we give up on strong consistency. We note that we have already proceeded likewise in [EOARD3], and that we were able to prove there, in some cases, that the method is convergent despite the absence of consistency.

1.2.4 Stab-Adv-MsFEM variant

In echo to the variant described in Section 1.2.3, it may be interesting to also consider a stabilized version of the Adv-MsFEM variant introduced in Section 1.2.1. The problem consists in finding $u_H^{\varepsilon} \in V_H^{\varepsilon,Adv}$ such that

$$\forall v_H^{\varepsilon} \in V_H^{\varepsilon,Adv},\quad \mathcal{A}_{\varepsilon}^{H}(u_H^{\varepsilon}, v_H^{\varepsilon}) + \mathcal{A}_{\mathrm{stab}}(u_H^{\varepsilon}, v_H^{\varepsilon}) = F_{\varepsilon}(v_H^{\varepsilon}) + F_{\mathrm{stab}}(v_H^{\varepsilon}),\quad (19)$$

where $V_H^{\varepsilon,Adv}$ is defined by (9) and $\mathcal{A}_{\mathrm{stab}}$ and F_{stab} are defined as in (14)–(15).

16

In practice, we again only know discrete approximations $\Psi_h^{\varepsilon,\mathbf{K}}$ and $\Phi_h^{\varepsilon,E}$, on a fine mesh $\mathbf{K}_h$, of the solutions $\Psi^{\varepsilon,\mathbf{K}}$ and $\Phi^{\varepsilon,E}$ to (7) and (8), respectively. The term $\mathcal{A}_{\text{stab}}(u_{H,h}^\varepsilon, v_{H,h}^\varepsilon)$ is again ill-defined. We proceed as for the Stab-MsFEM variant (see (18)) and consider the following variational formulation: find $u_{H,h}^\varepsilon \in V_{H,h}^{\varepsilon,Adv}$ such that

$$\forall v_{H,h}^\varepsilon \in V_{H,h}^{\varepsilon,Adv}, \quad \mathcal{A}_\varepsilon^H(u_{H,h}^\varepsilon, v_{H,h}^\varepsilon) + \mathcal{A}_{\text{upw}}(u_{H,h}^\varepsilon, v_{H,h}^\varepsilon) = F_\varepsilon(v_{H,h}^\varepsilon) + F_{\text{stab}}(v_{H,h}^\varepsilon),$$

where

$$\mathcal{A}_{\text{upw}}(u_{H,h}^\varepsilon, v_{H,h}^\varepsilon) = \sum_{\mathbf{K}\in\mathcal{T}_H} U_\mathbf{K} \int_{\mathbf{K}\cap\Omega_\varepsilon} \tau_\mathbf{K}(x) \left(\frac{b(x/\varepsilon)}{\varepsilon} \cdot \nabla v_{H,h}^\varepsilon \right)$$

with $u_{H,h}^\varepsilon(x) = \displaystyle\sum_{E\in\mathcal{E}_H} U_E \, \Phi_h^{\varepsilon,E}(x) + \sum_{\mathbf{K}\in\mathcal{T}_H} U_\mathbf{K} \, \Psi_h^{\varepsilon,\mathbf{K}}(x).$

1.3 Numerical results

We describe here some preliminary numerical tests, and refer to [EOARD4] for more comprehensive results.

We consider problem (1) in dimension $d = 2$. The perforated domain is $\Omega_\varepsilon = \Omega \setminus \overline{B_\varepsilon}$, where $\Omega = (0,1)^2$ and B_ε is the set of squares of sidelength 0.5ε periodically located on the regular grid of period ε. We consider the generic case when the mesh edges intersect the perforations. Unless otherwise stated, we set $b = (1,1)^T$ and $f = 1$. The parameters ε and α will be specified along the different numerical results.

We focus on the relative error in the H^1 norm, which is defined, for any numerical solution v, by

$$e(v) = \frac{\sqrt{\sum_{\mathbf{K}\in\mathcal{T}_H} \|v - u_{\text{ref}}\|_{H^1(\mathbf{K}\setminus\overline{B_\varepsilon})}^2}}{\|u_{\text{ref}}\|_{H^1(\Omega_\varepsilon)}}, \tag{20}$$

where u_{ref} is the reference solution, which has been computed by directly solving (1) on a very fine mesh.

1.3.1 Comparison of the MsFEM approaches

We compare the four variants we have introduced, namely the MsFEM (see Section 1.2.2), the Stab-MsFEM (see Section 1.2.3), the Adv-MsFEM (see Section 1.2.1) and the Stab-Adv-MsFEM (see Section 1.2.4). All the methods share comparable offline costs, and identical online cots.

17

We first investigate the sensitivity to the coarse mesh size H. We thus fix $\alpha = 1/4$, $\varepsilon = 1/0.03$ and let H vary. We plot the errors on Figure 6. We observe that the stabilization is not useful (in the sense that the methods with or without the stabilization terms yield similar results), and that the Adv-MsFEM method provides more accurate results than the MsFEM method.
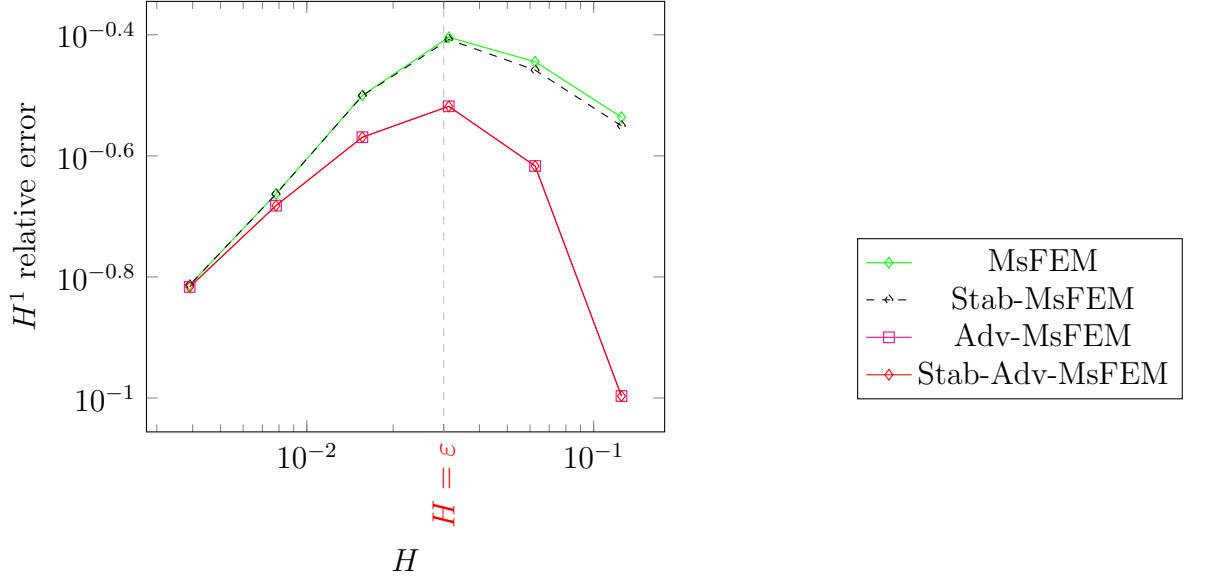

Figure 6: Relative error (20) for the 4 numerical variants ($\alpha = 1/4$, $\varepsilon = 0.03$; the vertical dashed line represents the region where $H = \varepsilon$).

We next investigate the influence of the parameter α, which measures the relative importance of the diffusion and the convection in the problem. We fix $H = 1/16$, $\varepsilon = 1/32$ and let α in (1) vary. We plot the errors on Figure 7. Again, the stabilization does not appear to be useful, and the Adv-MsFEM method provides more accurate results than the MsFEM method.

We eventually examine the robustness of the approaches to the small scale ε present in the problem. MsFEM approaches are indeed supposed to provide accurate results for fixed H even if ε is asymptotically small, in contrast to standard FEM approaches. We set $f(x,y) = \sin\left(\dfrac{\pi x}{2}\right)\sin\left(\dfrac{\pi y}{2}\right)$, $H = 1/16$, $\alpha = 1/16$ and let ε vary. As for the previous tests, we observe on Figure 8 that
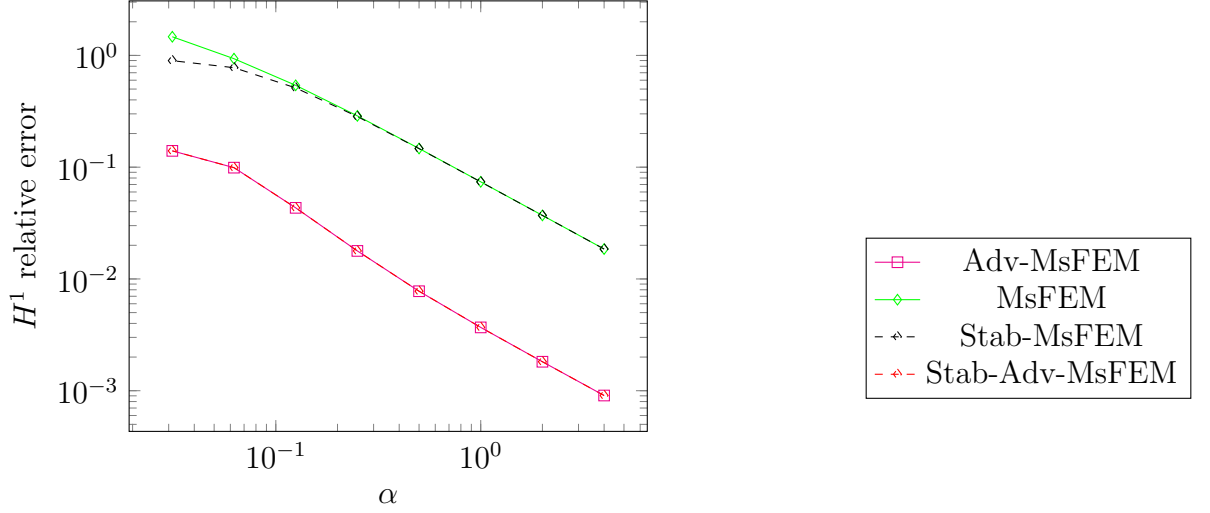
18

Figure 7: Relative error (20) for the 4 numerical variants ($\varepsilon = 1/32$, $H = 1/16$).

the Adv-MsFEM and the Stab-Adv-MsFEM methods provide more accurate results than the MsFEM and the Stab-MsFEM methods.

1.4 Conclusions and perspectives

Our first numerical tests show that the Adv-MsFEM and the Stab-Adv-MsFEM approaches provide solutions with the best accuracy, in term of H^1 error over the whole domain Ω_ε. However, our results are only preliminary, and much remains to be understood.

For instance, to have a better understanding of the different numerical approaches, we wish to investigate the question of where in Ω_ε the error is essentially located. This is a delicate question. For MsFEM approaches, the error typically comes from a mismatch between the exact solution and the numerical solution close to the edges of the coarse mesh (thus the introduction of the popular oversampling variant, ...). However, for convection-dominated problems, the situation can be different. For instance, we considered in [EOARD3] a multiscale convection-dominated problem, for which all numerical approaches produced large errors (overshadowing the error at the coarse mesh edges) in a boundary layer due to the strong convection. For the problem considered here,

19
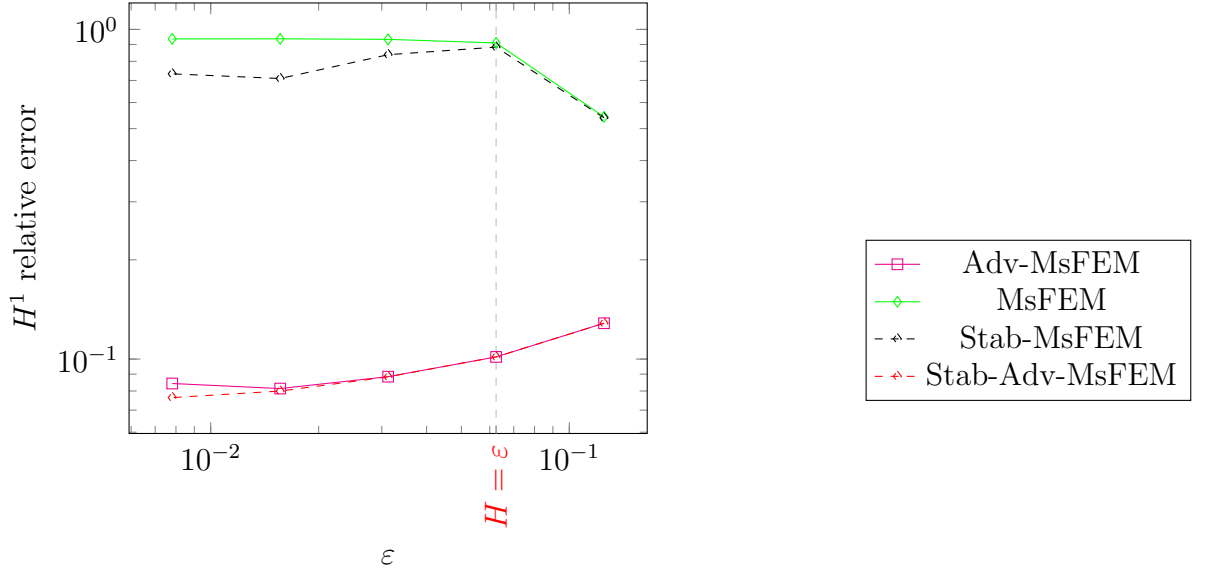
Figure 8: Relative error (20) for the 4 numerical variants ($\alpha = 1/16$, $H = 1/16$).

which is convection-dominated and set on a perforated domain, the situation might be again different. This question thus has to be investigated in details.

Another question we wish to study is to better understand why the Adv-MsFEM approach appears here to be the best, whereas it used to be outperformed by the Stab-MsFEM approach in the work [EOARD3]. Note that criteria of performance are different in both cases: the H^1 error in the former case, the H^1 error *outside a boundary layer* in the latter case (due to the fact that, as pointed out above, all numerical approaches produced large errors in the boundary layer).

It also remains to understand whether the Stab-Adv-MsFEM approach provides systematically better results than the Adv-MsFEM approach. If not, then the Adv-MsFEM approach appears to be the method of choice, since it provides accurate results and does not require the assembling of stabilization terms.

All these questions will be investigated in [EOARD4].

20

2 Construction of coarse approximations for problems with highly oscillatory coefficients

The work we now describe addresses the construction of coarse approximations for problems with highly oscillatory coefficients. It has been completed in collaboration with Simon Lemaire, a postdoc student fully funded by this Grant from June 1st, 2014 until September 30th, 2015.

Consider an heterogeneous material, modelled by highly oscillatory coefficients, which we denote here by A^ε. For simplicity, we assume that A^ε is a symmetric matrix. The question we investigate is to find the best non-oscillating coefficient $\overline{A}$ (think e.g. of a constant coefficient) that is consistent, in a sense to be made precise, with the behavior of the heterogeneous material modelled by A^ε. Put differently, we wish to approximate the solution u^ε to the problem

$$-\operatorname{div}\left[A^\varepsilon(x)\nabla u^\varepsilon\right] = f \ \text{ in } \Omega, \qquad u^\varepsilon = 0 \ \text{ on } \partial\Omega, \tag{21}$$

using a similar problem with a *constant* coefficient $\overline{A}$, which reads

$$-\operatorname{div}\left[\overline{A}\,\nabla\overline{u}\right] = f \ \text{ in } \Omega, \qquad \overline{u} = 0 \ \text{ on } \partial\Omega. \tag{22}$$

We want the approximation to be accurate for ideally all right hand sides f.

The motivation for this approach is to find a pathway alternative to standard homogenization techniques when these latter are difficult to use in practice. Indeed, homogenization theory (and the numerical homogenization techniques, such as MsFEM, that derive from it) requires a complete knowledge of the oscillatory coefficient A^ε (e.g. to compute the multiscale basis functions in (7)–(8)). In many practical cases, this coefficient is only partially known, or one only has access to the solution of (21) for some loadings f.

When ε is asymptotically small, $\overline{A}$ should then be a good approximation of the homogenized matrix $A_\star$. This is indeed the case for the two formulations, see (23), (24) and (25) below, that we have considered (see [5, EOARD1]). The approach can thus be employed to approximate $A_\star$. However, the most interesting regime is when ε is small but not asymptotically small. Our approach provides a way to approximate the solution $u^\varepsilon(f)$ to (21) (which is expensive to compute, especially in a multi-query context where several f have to be considered) by the solution $\overline{u}(f)$ to (22), which can be computed in an inexpensive way as soon as $\overline{A}$ has been identified. Besides $A_\star$ or $u^\varepsilon(f)$, another quantity of interest is $\nabla u^\varepsilon(f)$. We examine below how to approximate these quantities.

2.1 A quadratic optimization formulation

A central question is to construct in an efficient manner the best constant coefficient $\overline{A}$ approximating the oscillatory problem. We have addressed this question in [5], where we have considered the following optimization problem:

$$\inf_{\text{symmetric matrix } \overline{A}} \quad \sup_{f \in L^2(\Omega), \ \|f\|_{L^2(\Omega)} = 1} \quad J_\varepsilon(\overline{A}, f) \tag{23}$$

with

$$J_\varepsilon(\overline{A}, f) = \|u^\varepsilon(f) - \overline{u}(\overline{A}, f)\|_{L^2(\Omega)}^2 \tag{24}$$

where $u^\varepsilon(f)$ is the solution to (21) with the right-hand side f and $\overline{u}(\overline{A}, f)$ is the solution to (22) with the right-hand side f and the constant matrix $\overline{A}$. However, this problem is difficult to solve, because it is *nonconvex*. As pointed out in the previous EOARD report [EOARD6], we have recently investigated a different formulation of the problem. It is given by (23), where now we take

$$J_\varepsilon(\overline{A}, f) = \left\|(-\Delta)^{-1}\Big(\operatorname{div}(\overline{A}\nabla u^\varepsilon(f)) + f\Big)\right\|_{L^2(\Omega)}^2, \tag{25}$$

where $u^\varepsilon(f)$ is the unique solution to (21) and the operator $(-\Delta)^{-1}$ is defined by

$$w = (-\Delta)^{-1}g \quad \text{when} \quad -\Delta w = g \ \text{ in } \Omega \ \text{ and } \ w = 0 \ \text{ on } \partial\Omega.$$

Note that the cost function (25) is related to (24) through the application, inside the L^2 norm, of the operator $(-\Delta)^{-1}\Big(\operatorname{div}(\overline{A}\nabla\cdot)\Big)$.

We emphasize that (25) is quadratic with respect to f and $\overline{A}$, in contrast to (24). The problem (23)–(25) thus has the advantage of being *convex*. This is of paramount importance for the efficiency of the numerical approach [EOARD1].

2.1.1 Algorithm to solve (23)–(25)

An algorithm to solve (23)–(25) has been presented in the previous EOARD report [EOARD6]. We simply recall here that the supremum over $f \in L^2(\Omega)$ in (23) is approximated by a supremum in a finite-dimensional space. More precisely, problem (23) is approximated by

$$\inf_{\text{symmetric matrix } \overline{A}} \quad \sup_{f \in V_P, \ \|f\|_{L^2(\Omega)} = 1} \quad J_\varepsilon(\overline{A}, f), \tag{26}$$

22

where V_P is the finite dimensional space generated by the first P eigenfunctions of the laplacian operator on Ω, that is

$$V_P = \text{Span}\left\{f_p, \ 1 \leq p \leq P\right\}, \tag{27}$$

where $-\Delta f_p = \lambda_p f_p$ on Ω with $f_p = 0$ on $\partial\Omega$. We normalize the functions f_p so that $\int_\Omega f_p f_q = \delta_{qp}$.

2.1.2 Adaptation to the random setting

We have presented in the previous EOARD report [EOARD6] some preliminary numerical results in a periodic case. In this report, we focus on the stationary random case. Our approach is adapted to that context by simply considering (26), where $J_\varepsilon(\overline{A}, f)$ is now given by

$$J_\varepsilon(\overline{A}, f) = \left\| (-\Delta)^{-1}\Big(\text{div}\left(\overline{A}\nabla \mathbb{E}\left[u^\varepsilon(f)\right]\right) + f \Big) \right\|_{L^2(\Omega)}^2, \tag{28}$$

where $u^\varepsilon(\omega, f)$ is the unique solution to

$$-\text{div}\left[A\left(\frac{x}{\varepsilon}, \omega\right)\nabla u^\varepsilon\right] = f \ \text{ in } \Omega, \qquad u^\varepsilon = 0 \ \text{ on } \partial\Omega, \tag{29}$$

where the matrix A is random and stationary (i.e. statistically homogeneous).

In practice, the expectation in (28) is approximated by an empirical mean over M i.i.d. realizations:

$$\mathbb{E}\left[u^\varepsilon(f)\right] \approx \frac{1}{M}\sum_{m=1}^{M} u^\varepsilon(\omega_m, f).$$

Problem (26) is thus approximated by

$$
\begin{cases}
\displaystyle \inf_{\text{symmetric matrix } \overline{A}} \ \sup_{f \in V_P, \ \|f\|_{L^2(\Omega)}=1} J_\varepsilon^M(\overline{A}, f), \\[2ex]
\displaystyle J_\varepsilon^M(\overline{A}, f) = \left\| (-\Delta)^{-1}\left(\text{div}\left(\frac{\overline{A}}{M}\nabla\left[\sum_{m=1}^{M} u^\varepsilon(\omega_m, f)\right]\right) + f \right) \right\|_{L^2(\Omega)}^2.
\end{cases} \tag{30}
$$

In the sequel, we compare our approach with the standard homogenization approach, which reads as follows. The solution $u^\varepsilon(\cdot, \omega)$ to (29) converges, when $\varepsilon \to 0$, to $u_\star$, solution to the homogenized problem

$$-\text{div}\left[A_\star \nabla u_\star\right] = f \ \text{ in } \Omega, \qquad u_\star = 0 \ \text{ on } \partial\Omega, \tag{31}$$

23

where the homogenized matrix $A_\star$ is constant and deterministic. This matrix is challenging to compute, and in practice approximated as follows. Consider the truncated corrector equation

$$-\operatorname{div}\left(A(\cdot,\omega)(\boldsymbol{p}+\boldsymbol{\nabla} w_{\boldsymbol{p}}^N(\cdot,\omega))\right)=0 \quad \text{in } Q^N, \qquad w_{\boldsymbol{p}}^N(\cdot,\omega) \text{ is } Q^N\text{-periodic}, \quad (32)$$

posed on a large domain $Q^N = (-N,N)^d$, where $\boldsymbol{p} \in \mathbb{R}^d$ is a constant. We then compute the random matrix $A_\star^N(\omega)$ defined by

$$\left[A_\star^N(\omega)\right]_{i,j} = \frac{1}{|Q^N|} \int_{Q^N} \left(\boldsymbol{e}_i + \boldsymbol{\nabla} w_{\boldsymbol{e}_i}^N(\cdot,\omega)\right)^T A(\cdot,\omega) \left(\boldsymbol{e}_j + \boldsymbol{\nabla} w_{\boldsymbol{e}_j}^N(\cdot,\omega)\right), \quad (33)$$

where $\{\boldsymbol{e}_i\}_{1\le i\le d}$ is the canonical basis of $\mathbb{R}^d$. It is well-known (see e.g. [4]) that $A_\star^N(\omega)$ almost surely converges, when $N \to +\infty$, to $A_\star$. Since $A_\star^N(\omega)$ is random, it is natural to consider M independent and identically distributed (i.i.d.) realizations of the field A, say $\{A(\cdot,\omega_m)\}_{1\le m\le M}$, solve (32) and compute (33) for each of them, and define

$$A_\star^{N,M} = \frac{1}{M} \sum_{m=1}^{M} A_\star^N(\omega_m) \qquad (34)$$

as a practical approximation to $A_\star$.

2.1.3 Approximation of u^ε in the H^1-norm

We have pointed out above that our approach yields a matrix $\overline{A}_\varepsilon$ which is a converging approximation of $A_\star$. The solution to (22) with $\overline{A} \equiv \overline{A}_\varepsilon$, which we denote $\overline{u}(\overline{A}_\varepsilon)$, is thus a converging approximation (in the H^1 norm, and thus in the L^2 norm) of $u_\star$. Since $u^\varepsilon(\cdot,\omega)$ converges (in the L^2 norm) to $u_\star$, we therefore see that our approach allows us to obtain a converging approximation of $u^\varepsilon(\cdot,\omega)$. However, in the H^1 norm, $u^\varepsilon(\cdot,\omega)$ is not close to $u_\star$, and hence $u^\varepsilon(\cdot,\omega)$ and $\overline{u}(\overline{A}_\varepsilon)$ are not close to each other.

We explain here how our approach can be complemented to obtain an approximation of $\mathbb{E}\left[u^\varepsilon\right]$ in the H^1-norm.

In many settings of homogenization theory (and in particular in the random setting we consider here), once the corrector problems (in practice, problems (32)) are solved to compute the homogenized matrix, the first-order two-scale expansion approximates u^ε in the H^1-norm. Consider indeed the function

$$u^{\varepsilon,1}(\boldsymbol{x},\omega) = u_\star(\boldsymbol{x}) + \varepsilon \sum_{i=1}^{d} w_{\boldsymbol{e}_i}\left(\frac{\boldsymbol{x}}{\varepsilon},\omega\right) \frac{\partial u_\star}{\partial x_i}(\boldsymbol{x}),$$

24

where $w_{\boldsymbol{e}_i}$ is the unique solution with vanishing mean value to the corrector equation for $\boldsymbol{p} = \boldsymbol{e}_i$. It is known that, in average, $u^\varepsilon - u^{\varepsilon,1}$ converges to 0 in the H^1 norm, in the sense that (see [6, Theorem 3])

$$\lim_{\varepsilon\to 0} \mathbb{E}\left[\left\|u^\varepsilon(\cdot,\omega) - u^{\varepsilon,1}(\cdot,\omega)\right\|_{H^1(\Omega)}^2\right] = 0.$$

This implies that

$$\mathbb{E}\left[\boldsymbol{\nabla} u^\varepsilon(\cdot,\omega)\right] = C_\varepsilon\,\boldsymbol{\nabla} u_\star + \text{h.o.t.}, \tag{35}$$

where C_ε is a $d \times d$ oscillatory matrix field given by, for any $1 \le i,j \le d$,

$$[C_\varepsilon]_{i,i} = 1 + \mathbb{E}\left[\partial_i w_{\boldsymbol{e}_i}(\cdot/\varepsilon,\omega)\right], \qquad [C_\varepsilon]_{i,j} = \mathbb{E}\left[\partial_i w_{\boldsymbol{e}_j}(\cdot/\varepsilon,\omega)\right] \quad \text{if } j \ne i. \tag{36}$$

Our idea for constructing an approximation of $\mathbb{E}\left[\boldsymbol{\nabla} u^\varepsilon\right]$ is to mimick formula (35) and seek an approximation under the form $\overline{C}_\varepsilon \boldsymbol{\nabla}\overline{u}_\varepsilon$, where $\overline{u}_\varepsilon \equiv \overline{u}(\overline{A}_\varepsilon)$. Once the best matrix $\overline{A}_\varepsilon$ has been computed, we compute a surrogate $\overline{C}_\varepsilon$ of C_ε by solving the least-squares problem

$$\inf_{\overline{C}\in(L^2(\Omega))^{d\times d}} \sum_{r=1}^R \left\|\boldsymbol{\nabla}\mathbb{E}\left[u_\varepsilon(f_r)\right] - \overline{C}\,\boldsymbol{\nabla}\overline{u}_\varepsilon(f_r)\right\|_{L^2(\Omega)^d}^2 \tag{37}$$

for a given number R of right-hand sides.

In practice, the expectation in (37) is approximated by a mean over M realizations, and the right-hand sides f_r selected for (37) are the first R basis functions of the space V_P defined by (27), with R such that

$$R \le P.$$

The fact that we consider a number $R \le P$ of right-hand sides makes the H^1-reconstruction an inexpensive post-processing procedure once the best matrix is computed, as we already have at our disposal $u_\varepsilon(\omega, f_r)$ for $1 \le r \le R$.

The tensor $\overline{C}$ is discretized as a piecewise constant function on a fine mesh. Solving (37) hence amounts to solving many least-squares problems (independent one from each other) set in a $d \times d$ dimensional space (as $\overline{C}$ is a $d \times d$ matrix). The associated cost is negligible in comparison to the cost for computing the solutions to (29) that are needed in (30).

2.2 Numerical results

We work in dimension $d = 2$, with $\Omega = (0,1)^2$. We consider the random checkerboard test-case, namely

$$A_\varepsilon(x, y, \omega) = a^{\mathrm{sta}}(x/\varepsilon, y/\varepsilon, \omega) \,\mathrm{Id}_2, \qquad (38)$$

with a^{sta} given by

$$a^{\mathrm{sta}}(x, y, \omega) = \sum_{\boldsymbol{k} \in \mathbb{Z}^2} 1_{Q+\boldsymbol{k}}(x, y) X_{\boldsymbol{k}}(\omega), \qquad (39)$$

where $Q = (0,1)^2$ and where the random variables $X_{\boldsymbol{k}}$ are i.i.d. and such that $\mathbb{P}(X_{\boldsymbol{k}} = 4) = \mathbb{P}(X_{\boldsymbol{k}} = 16) = 1/2$. An explicit expression for the homogenized matrix is known in that case (of course, our approach does not use that knowledge):

$$A_\star = 8 \,\mathrm{Id}_2. \qquad (40)$$

In what follows, we only consider the case of small values of ε in (29) (namely, $\varepsilon < |\Omega|^{1/2}/10 = 0.1$). We refer to [EOARD1] for comprehensive results.

In short, the numerical experiments reported below show that the approximation of $A_\star$ obtained by the classical homogenization approach is slightly more accurate than the one obtained with our approach. In contrast, our approach provides a better L^2-approximation and a better H^1-approximation. In terms of computational cost, our approach is less expensive for moderately small values of ε, and more expensive for asymptotically small values of ε.

2.2.1 Cost comparison to the standard homogenization approach

For asymptotically small values of ε, our method can be seen as a practical approach to compute the homogenized matrix $A_\star$. The question is whether this approach is efficient, in comparison with the classical approach in random homogenization. As recalled above, this latter approach requires solving the equations (32), set on $Q^N = (-N, N)^d$. The coefficients of (32) vary at scale 1. In that case, to hope for an accurate approximation, one has to consider a meshsize $H \ll 1$. In our approach, we need to solve (29), where the coefficients vary at scale ε. To that aim, we use a mesh of size h. We choose h and H such that

$$\frac{\varepsilon}{h} = \frac{1}{H}, \qquad (41)$$

26

hoping thus for a similar accuracy when solving (29) or (32).

We see that, up to an appropriate choice of the parameter H such that

$$\left(\frac{2N}{H}\right)^d = \frac{\text{size}(\Omega)}{h^d}, \tag{42}$$

both the standard homogenization approach and our approach require solving linear systems of the same size. The computational workload for the two approaches is thus of the same order of magnitude, although not identical. In the sequel, we have enforced (42) and (41), which imply that N in (32) and ε in (29) are related by

$$N = \text{size}(\Omega)/2\varepsilon. \tag{43}$$

For the two methods, the same number M of Monte Carlo realizations is used, and the same M realizations are considered.

For the standard approach in homogenization, we denote by $A_{\star,H}^{N,M}$ the practical approximation of $A_\star^{N,M}$ defined in (34). Our approach consists in computing the best matrix $\overline{A}_{\varepsilon,h}^{P,M}$ following (30). Recall that P denotes the dimension of the set V_P used to approximate the space L^2 in the sup problem (see (27)). In the sequel, we take $P = 3$.

We first comment on the CPU times (see Figure 9), namely the time needed to compute either $A_{\star,H}^{N,M}$ by standard random homogenization or $\overline{A}_{\varepsilon,h}^{P,M}$ using our approach. To perform that comparison, we make use of an implementation that does not exploit parallelism, and we solve the linear systems by means of an iterative solver. In view of Figure 9, our method is slightly faster than standard random homogenization for values of N up to approximately 14.

This observation can be explained as follows. For the number $M = 100$ of Monte Carlo realizations that we consider, we can neglect, in our procedure, the cost of optimization in comparison to the cost of computing the solutions $u^\varepsilon(\omega_m, f_p)$ to (29), for $1 \le m \le M$ and $1 \le p \le P$. Hence, to compute $\overline{A}_{\varepsilon,h}^{P,M}$, we have to (i) assemble $M = 100$ stiffness matrices, (ii) assemble $P = 3$ right-hand sides, and (iii) solve $P \times M = 300$ linear systems. In contrast, to compute $A_{\star,H}^{N,M}$, one has to solve $d \times M = 200$ approximate corrector equations (32), that is to say (i) assemble $M = 100$ stiffness matrices, (ii) assemble $d \times M = 200$ right-hand sides, and (iii) solve $d \times M = 200$ linear systems. Consequently, on the one hand, our approach necessitates solving 100 more linear systems than the standard homogenization approach, but on the other hand, the standard

27

approach necessitates assembling approximately 200 more right-hand sides than our approach. This explains what we observe. When the value of N is not too large, the assembly cost is higher than the inversion cost, and our approach is faster.
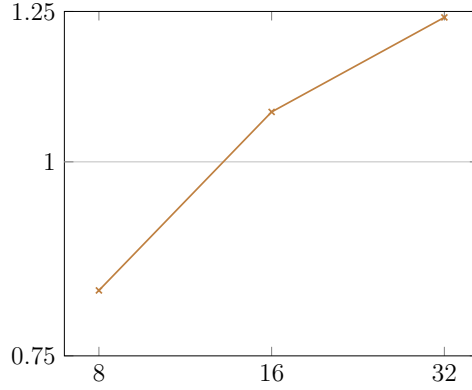

Figure 9: Ratio between the CPU time needed by our approach and the CPU time needed by the standard approach in random homogenization in function of N, for $M = 100$.

2.2.2 Approximation of $A_\star$

We consider the parameters $(N_k)_{3 \leq k \leq 5}$ (defining the domain on which we solve the corrector problems (32)) such that $N_k = 2^k$. In agreement with (43), this implies that the small scale present in (29) is given by $(\varepsilon_k)_{3 \leq k \leq 5}$ such that $\varepsilon_k = 2^{-(k+1)}$. The associated meshsizes $(h_k)_{3 \leq k \leq 5}$ and $(H_k)_{3 \leq k \leq 5}$ are computed respectively letting $h_k = \varepsilon_k/r$ for $r = 27$, $r = 54$ or $r = 108$ and using (42). We consider $M = 100$ Monte Carlo realizations.

The error in the approximation of the homogenized matrix is defined, for $\widehat{A}^M \in \left\{ A_{\star,H}^{N,M}, \overline{A}_{\varepsilon,h}^{P,M} \right\}$, by

$$
\texttt{err\_mat} = \left(\frac{\sum_{1 \leq i,j \leq d} \left| \left[\widehat{A}^M \right]_{i,j} - [A_\star]_{i,j} \right|^2}{\sum_{1 \leq i,j \leq d} |[A_\star]_{i,j}|^2} \right)^{1/2},
$$

where $A_\star$ is taken equal to the exact value (40).

28

The numerical results are collected in Figure 10. We observe that the matrix $\overline{A}_{\varepsilon,h}^{P,M}$ provided by our approach converges to the homogenized matrix as $N = 1/(2\varepsilon)$ grows. However, for any value of N in the range we consider, the approximation of $A_\star$ obtained with the usual approach is slightly more accurate (and less expensive when $N \geq 14$, see Figure 9) than the one obtained with our approach.
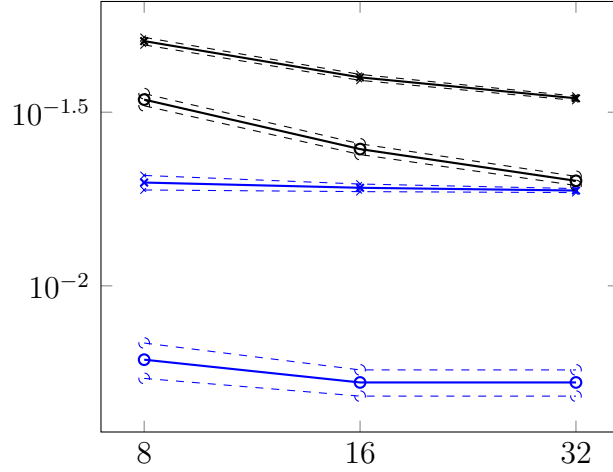

Figure 10: Approximation of $A_\star$ by standard random homogenization (blue) and by our approach (black) in function of N, for $M = 100$ realizations. Since M is finite, we compute the error `err_mat` 100 times. The thick line corresponds to the mean value over the 100 computations of the error. The dashed lines show the 95% confidence interval. Results obtained with h such that $\varepsilon/h = 27$ (resp. $\varepsilon/h = 108$) are denoted with x (resp. o).

2.2.3 Approximation of u^ε in the L^2 norm

We denote by

- $u_{\varepsilon,h}^M(f)$ the empirical expectation, defined by

$$u_{\varepsilon,h}^M(f) = \frac{1}{M} \sum_{m=1}^{M} u_{\varepsilon,h}(\omega_m, f), \qquad (44)$$

  of the discrete solutions to (29) with oscillatory coefficients given by (38)–(39) and right-hand side f;

29

- $u_{\star,h}(f)$ the discrete solution to (31) with exact matrix (40) and right-hand side f (note that the exact homogenized matrix $A_\star$ is usually unknown);

- $u_{\star,h}^{N,M}(f)$ the discrete solution to (31) with matrix $A_{\star,H}^{N,M}$ and right-hand side f;

- $\overline{u}_{\varepsilon,h}^{P,M}(f)$ the discrete solution to (22) with matrix $\overline{A}_{\varepsilon,h}^{P,M}$ and right-hand side f.

So as to assess the quality of the approximation of $\mathbb{E}[u^\varepsilon]$ by

$$\widehat{u}_h(f) \in \left\{ u_{\star,h}(f),\ u_{\star,h}^{N,M}(f),\ \overline{u}_{\varepsilon,h}^{P,M}(f) \right\}$$

in the L^2 norm, we define the criterion

$$\texttt{err\_l2} = \left(\frac{\displaystyle\sup_{f \in V_\mathcal{Q}} \left\| u_{\varepsilon,h}^M(f) - \widehat{u}_h(f) \right\|_{L^2(\Omega)}^2}{\left\| u_{\varepsilon,h}^M(\widehat{f}_\varepsilon) \right\|_{L^2(\Omega)}^2} \right)^{1/2},$$

where $\widehat{f}_\varepsilon \in V_\mathcal{Q}$ denotes the argument of the sup problem in the numerator. Note that the supremum is taken over $f \in V_\mathcal{Q}$ with $\mathcal{Q} \gg P$. We take $\mathcal{Q} = 16$, and we have checked that our results do not change for a larger value of $\mathcal{Q}$.

The numerical results are collected in Figure 11. We observe that the solution $\overline{u}_{\varepsilon,h}^{P,M}(f)$ provided by our approach is a better L^2-approximation (for the range of parameters considered here) of $\mathbb{E}(u_\varepsilon)$ than the solutions associated with the exact or approximate homogenized matrices. Due to the small number of right-hand sides we consider to compute $\overline{A}_{\varepsilon,h}^{P,M}$, this good accuracy is not an immediate consequence of our practical procedure. We also observe that the accuracy of the three approximations $u_{\star,h}$, $u_{\star,h}^{N,M}$ and $\overline{u}_{\varepsilon,h}^{P,M}$ improves when h decreases or when M increases, in somewhat a complex manner. In terms of cost, our approach is again less expensive than the classical approach for $N \leq 14$.

2.2.4 Approximation of u^ε in the H^1 norm

We eventually turn to the H^1-error. We denote by $C_{\varepsilon,h}^{N,M}$ the practical approximation of the deterministic oscillatory matrix C_ε defined by (36) by an empirical mean over M realizations of the truncated corrector functions, solutions to (32):

$$\left[C_{\varepsilon,h}^{N,M} \right]_{ij} = \delta_{ij} + \frac{1}{M} \sum_{m=1}^{M} \partial_i w_{\boldsymbol{e}_j}^N(\cdot/\varepsilon, \omega_m).$$
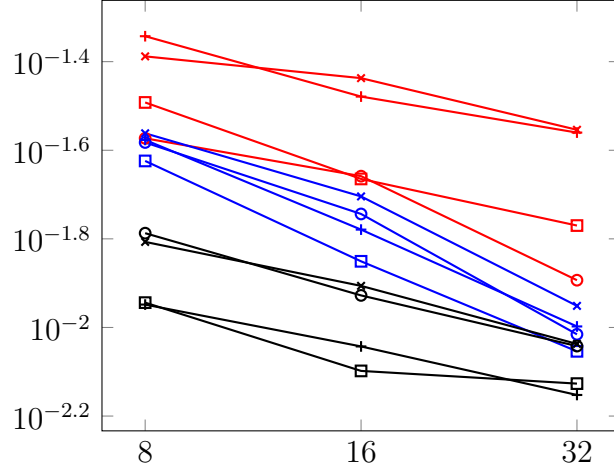
30

Figure 11: Approximation of $\mathbb{E}(u_\varepsilon)$ in the L^2-norm (`err_l2`) by $u_{\star,h}$ (red), $u_{\star,h}^{N,M}$ (blue) and $\overline{u}_{\varepsilon,h}^{P,M}$ (black) in function of N (curves with x: $\varepsilon/h = 27$ and $M = 100$; curves with o: $\varepsilon/h = 108$ and $M = 100$; curves with +: $\varepsilon/h = 27$ and $M = 400$; curves with □: $\varepsilon/h = 54$ and $M = 400$).

For $f \in L^2(\Omega)$, we denote by $C_{\varepsilon,h}^{N,M} \boldsymbol{\nabla} u_{\star,h}(f)$ and $C_{\varepsilon,h}^{N,M} \boldsymbol{\nabla} u_{\star,h}^{N,M}(f)$ the two discrete equivalents of $C_\varepsilon \boldsymbol{\nabla} u_\star(f)$, the homogenization-based approximation of $\mathbb{E}\left(\boldsymbol{\nabla} u_\varepsilon(f)\right)$, obtained by using the exact homogenized matrix (40) and the matrix $A_{\star,H}^{N,M}$, respectively, to compute an approximation of $u_\star(f)$. In our approach, we seek a discrete approximation of $\mathbb{E}\left(\boldsymbol{\nabla} u_\varepsilon(f)\right)$ under the form $\overline{C}_{\varepsilon,h}^{R,M} \boldsymbol{\nabla} \overline{u}_{\varepsilon,h}^{P,M}(f)$, with $R = P = 3$ (see (37)). For

$$\widehat{C}_{\varepsilon,h}^{M} \boldsymbol{\nabla} \widehat{u}_h(f) \in \left\{ C_{\varepsilon,h}^{N,M} \boldsymbol{\nabla} u_{\star,h}(f), \ C_{\varepsilon,h}^{N,M} \boldsymbol{\nabla} u_{\star,h}^{N,M}(f), \ \overline{C}_{\varepsilon,h}^{R,M} \boldsymbol{\nabla} \overline{u}_{\varepsilon,h}^{P,M}(f) \right\},$$

we define the criterion

$$\texttt{err\_h1} = \left(\frac{\displaystyle\sup_{f \in V_\mathcal{Q}} \left\| \boldsymbol{\nabla} u_{\varepsilon,h}^{M}(f) - \widehat{C}_{\varepsilon,h}^{M} \boldsymbol{\nabla} \widehat{u}_h(f) \right\|_{L^2(\Omega)}^{2}}{\left\| \boldsymbol{\nabla} u_{\varepsilon,h}^{M}(\widehat{f}_\varepsilon) \right\|_{L^2(\Omega)}^{2}} \right)^{1/2}, \qquad (45)$$

where, here again, the supremum is taken over the space $V_\mathcal{Q}$ for $\mathcal{Q} = 16 \gg P$ and where $\widehat{f}_\varepsilon \in V_\mathcal{Q}$ denotes the argument of the sup problem. We recall that, in (45), $u_{\varepsilon,h}^{M}(f)$ is the empirical mean (44) over M realizations of $u_{\varepsilon,h}(f;\omega)$. It is thus an approximation to $\mathbb{E}\left[u_\varepsilon(f)\right]$.

31

The numerical results are collected in Table 1. Our surrogate defines an approximation of $\mathbb{E}(\boldsymbol{\nabla} u_\varepsilon)$ which is systematically more accurate than the one provided by the homogenization-based approach, for any h and M.

N	8	16	32
`err_h1` for $C_{\varepsilon,h}^{N,M}\boldsymbol{\nabla} u_{\star,h}$ $(\varepsilon/h = 27,\ M = 100)$	$1.043\ 10^{-1}$	$9.635\ 10^{-2}$	$9.394\ 10^{-2}$
$(\varepsilon/h = 108,\ M = 100)$	$8.648\ 10^{-2}$	$8.120\ 10^{-2}$	$8.010\ 10^{-2}$
$(\varepsilon/h = 27,\ M = 400)$	$8.542\ 10^{-2}$	$7.828\ 10^{-2}$	$7.298\ 10^{-2}$
$(\varepsilon/h = 54,\ M = 400)$	$6.599\ 10^{-2}$	$6.222\ 10^{-2}$	$6.067\ 10^{-2}$
`err_h1` for $C_{\varepsilon,h}^{N,M}\boldsymbol{\nabla} u_{\star,h}^{N,M}$ $(\varepsilon/h = 27,\ M = 100)$	$9.799\ 10^{-2}$	$9.095\ 10^{-2}$	$8.961\ 10^{-2}$
$(\varepsilon/h = 108,\ M = 100)$	$8.620\ 10^{-2}$	$8.022\ 10^{-2}$	$7.952\ 10^{-2}$
$(\varepsilon/h = 27,\ M = 400)$	$7.605\ 10^{-2}$	$7.173\ 10^{-2}$	$6.780\ 10^{-2}$
$(\varepsilon/h = 54,\ M = 400)$	$6.142\ 10^{-2}$	$5.957\ 10^{-2}$	$5.872\ 10^{-2}$
`err_h1` for $\overline{C}_{\varepsilon,h}^{R,M}\boldsymbol{\nabla}\overline{u}_{\varepsilon,h}^{P,M}$ $(\varepsilon/h = 27,\ M = 100)$	$6.000\ 10^{-2}$	$4.542\ 10^{-2}$	$3.018\ 10^{-2}$
$(\varepsilon/h = 108,\ M = 100)$	$5.912\ 10^{-2}$	$4.657\ 10^{-2}$	$3.596\ 10^{-2}$
$(\varepsilon/h = 27,\ M = 400)$	$3.030\ 10^{-2}$	$3.814\ 10^{-2}$	$2.625\ 10^{-2}$
$(\varepsilon/h = 54,\ M = 400)$	$5.157\ 10^{-2}$	$3.613\ 10^{-2}$	$2.849\ 10^{-2}$

Table 1: Approximation of $\mathbb{E}(\boldsymbol{\nabla} u_\varepsilon)$ in the L^2-norm (`err_h1`) by $C_{\varepsilon,h}^{N,M}\boldsymbol{\nabla} u_{\star,h}$, $C_{\varepsilon,h}^{N,M}\boldsymbol{\nabla} u_{\star,h}^{N,M}$ and $\overline{C}_{\varepsilon,h}^{R,M}\boldsymbol{\nabla}\overline{u}_{\varepsilon,h}^{P,M}$ in function of N (the various lines correspond to various values of h and M).

References[1]

[1] X. Blanc, C. Le Bris and P.-L. Lions, *A possible homogenization approach for the numerical simulation of periodic microstructures with defects*, Milan Journal of Mathematics, 80:351–367, 2012.

[2] X. Blanc, C. Le Bris and P.-L. Lions, *Local profiles and elliptic problems at different scales with defects*, C. R. Acad. Sci. Paris, Série I, 353:203–208, 2015.

[3] X. Blanc, C. Le Bris and P.-L. Lions, *Local profiles for elliptic problems at different scales: defects in, and interfaces between periodic structures*, Comm. P.D.E., 40(12): 2173-2236, 2015.

---

[1]References authored by the investigators in the context of the contract are listed in the Executive Summary.

[4] A. Bourgeat and A. Piatnitski, *Approximation of effective coefficients in stochastic homogenization*, Ann I. H. Poincaré - PR, 40(2):153–165, 2004.

[5] C. Le Bris, F. Legoll and K. Li, *Approximation grossière d'un problème elliptique à coefficients hautement oscillants (Coarse approximation of an elliptic problem with highly oscillatory coefficients)*, C. R. Acad. Sci. Paris, Série I, 351(7-8):265-270, 2013.

[6] G.C. Papanicolaou and S.R.S. Varadhan, *Boundary value problems with rapidly oscillating random coefficients*, Proc. Colloq. on Random Fields: Rigorous Results in Statistical Mechanics and Quantum Field Theory, vol. 10, North-Holland, 1981, pp. 835–873.